inorganics

MDPI

Article

Stabilization of ZrO_2 Powders via ALD of CeO_2 and ZrO_2

Chao Lin, Xinyu Mao, Tzia Ming Onn, Joonbaek Jang and Raymond J. Gorte *

Chemical and Biomolecular Engineering, University of Pennsylvania, Philadelphia, PA 19104, USA; linchao@seas.upenn.edu (C.L.); xinyumao@seas.upenn.edu (X.M.); tonn@seas.upenn.edu (T.M.O.); joonbaek@seas.upenn.edu (J.J.)

* Correspondence: gorte@seas.upenn.edu

Received: 30 August 2017; Accepted: 27 September 2017; Published: 3 October 2017

Abstract: ZrO_2 powders were modified by atomic layer deposition (ALD) with CeO_2 and ZrO_2, using $Ce(TMHD)_4$ and $Zr(TMHD)_4$ as the precursors, in order to determine the effect of ALD films on the structure, surface area, and catalytic properties of the ZrO_2. Growth rates were measured gravimetrically and found to be 0.017 nm/cycle for CeO_2 and 0.031 nm/cycle for ZrO_2. The addition of 20 ALD cycles of either CeO_2 or ZrO_2 was found to stabilize the surface area of the ZrO_2 powder following calcination to 1073 K and to suppress the tetragonal-to-monoclinic transition. Shrinkage of ZrO_2 wafers was also suppressed by the ALD films. When used as a support for Pd in CO oxidation, the CeO_2-modified materials significantly enhanced rates due to interactions between the Pd and the CeO_2. Potential applications for modifying catalyst supports using ALD are discussed.

Keywords: ALD; CeO_2; ZrO_2; CO oxidation; sintering; oxygen storage

1. Introduction

Ceria is an important catalytic material, both as an oxidation catalyst by itself and as a promoter when it is in contact with transition metals [1–6]. Because pure ceria loses its reducibility after high-temperature treatments or redox cycling [7–9], it is often used in the form of a mixed oxide with zirconia, especially in Three-Way Catalysts (TWC) employed in automotive emissions-control applications [10,11]. It is sometimes assumed that the role of zirconia in OSC is to maintain surface area, but ceria-zirconia phases maintain their reducibility upon redox cycling, even though they do not have substantially higher surface areas than would pure ceria under these conditions [11,12]. Indeed, oxygen binding in ceria-zirconia solid solutions has been shown to be weaker than oxygen binding in pure ceria [13–15].

There is evidence that interfacial contact between ceria and zirconia can influence properties of ceria even when the two oxides exist as separate phases. For example, it has been reported that most Ce ions at the interface of epitaxial ceria films on yttria-stabilized zirconia (YSZ) substrates exist as Ce^{3+} and that the average oxidation state is affected several nanometers from that interface [16]. In another report, ceria films on polycrystalline zirconia were shown to be much more reducible than ceria films on alumina [15]. Still another study of ceria films on YSZ single crystals found that the ceria particles tend to orient along specific crystallographic directions, suggesting strong interactions between the two phases [17].

In an attempt to take advantage of these interactions on high-surface-area catalysts, our laboratory recently investigated 0.4 nm conformal zirconia films on ceria powders using atomic layer deposition (ALD) [18]. In ALD, a substrate powder is first allowed to react with an organometallic precursor to a monolayer coverage, after which the adsorbed precursor is oxidized in a separate step. Conformal films of varying thickness are formed by repeating this cycle the desired number of times. The zirconia-on-ceria ALD study found that the surface areas and crystallite sizes of ALD-modified ceria

powders were dramatically stabilized against sintering to temperatures up to 1073 K [18]. Whereas the crystallite size of an unmodified ceria powder increased from 18 to 32 nm when the calcination temperature increased from 673 to 1073 K, the crystallite size of the ALD-modified ceria was unchanged by this treatment. The modified ceria also maintained its promotional effects for the water-gas-shift reaction when used as a support for Pd and showed improved tolerance to SO_2 poisoning.

Because the ALD film thicknesses in this previous study were much smaller than the crystallite sizes of the ceria powders that were stabilized, it is surprising that the zirconia film could have such a strong impact on crystallite stability. That, in turn, leads to questions about the mechanism of the stabilization and what effect film thickness and composition have on the results. Therefore, we set out to investigate the properties of ceria and zirconia powders following ALD of ceria and zirconia films. The present results show that both ceria and zirconia powders can be stabilized by zirconia ALD films, implying that there must be a physical aspect to the stabilization. ALD films appear to prevent surface diffusion of oxide cations, thus preventing sintering and crystallite growth. This could have important implications for the stabilization of catalysts.

2. Results and Discussion

The initial characterization of the deposition process for CeO_2 and ZrO_2 films on the ZrO_2 substrate involved measuring the sample mass as a function of the number of ALD cycles, as shown in Figure 1. For both CeO_2 and ZrO_2 deposition, the data demonstrate that the sample mass increased almost linearly with the number of ALD cycles. For CeO_2 deposition on ZrO_2, the mass increase after 20 cycles was 0.20 g/g ZrO_2. Assuming that the film grew uniformly over the 84 m^2/g ZrO_2 surface and had the bulk properties of CeO_2, this mass change corresponds to a growth rate of 0.017 nm/cycle. The deposition rate for ZrO_2 on ZrO_2 was higher, with the sample mass increasing by 0.30 g/g ZrO_2 after 20 cycles, corresponding to a deposition rate of 0.031 nm/cycle.

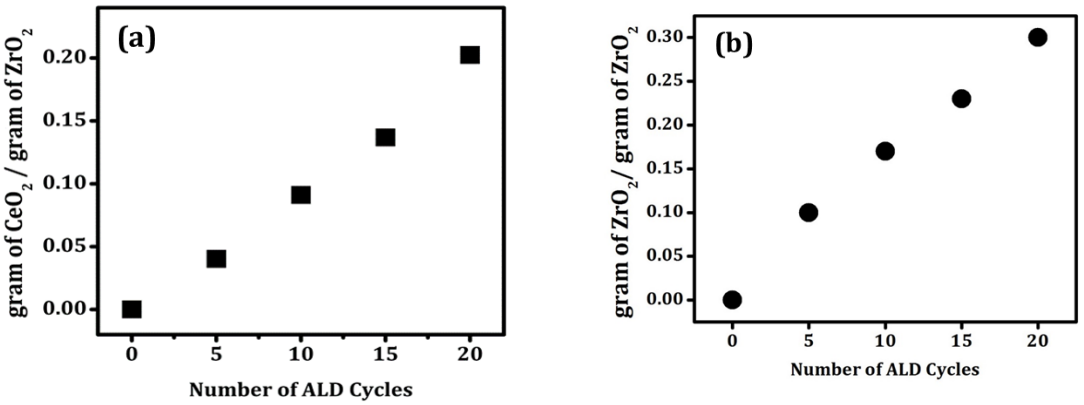

Figure 1. Growth curves for atomic layer deposition (ALD) films on an 84 m^2/g ZrO_2 powder: (**a**) CeO_2 ALD; (**b**) ZrO_2 ALD. All masses were measured after thermal treatment to ensure the removal of moisture content.

ALD of CeO_2 and ZrO_2 has been reported previously for a γ-Al_2O_3 substrate using the same organometallic precursors and similar deposition conditions [19]. In that study, the growth rates were 0.016 nm/cycle for CeO_2 and 0.024 nm/cycle for ZrO_2. Given the large differences in the nature of the ZrO_2 and γ-Al_2O_3 substrates used in these two studies, it is remarkable that the growth rates for both oxide films on both substrates were so similar. This suggests that the deposition process is primarily dictated by the organometallic precursors and not the substrate. On an atom basis, the deposition rates were 8.7×10^{17} Zr/m^2 cycle and 4.2×10^{17} Ce/m^2 cycle. These rates are much lower than one would expect if each cycle formed a monolayer oxide film, probably due to the large size of the THMD ligands in the organometallic precursors.

One of the most interesting observations from the previous ALD study of ZrO_2 on CeO_2 was that a 0.4 nm thick film, having a thickness that is smaller than the 0.52-nm lattice parameter of cubic zirconia, was able to stabilize the surface area and crystallite size of CeO_2 to high temperatures [18]. To better understand the effect of ALD films, we here investigated the influence of CeO_2 and ZrO_2 films on a ZrO_2 substrate as a function of film thickness. BET surface areas are reported as a function of calcination temperature in Table 1 for ZrO_2 samples that had been treated with 2, 10, or 20 ALD cycles of either CeO_2 or ZrO_2. The unmodified ZrO_2 sintered dramatically with temperature, with the surface area decreasing from 84 m^2/g after calcination at 773 K to only 20 m^2/g after heating to 1073 K.

Table 1. BET surface areas as a function of calcination temperature.

Calcination Temperature(K)	BET Surface Area (m^2/g)						
	ZrO_2	2 CeO_2/ZrO_2	10 CeO_2/ZrO_2	20 CeO_2/ZrO_2	2 ZrO_2/ZrO_2	10 ZrO_2/ZrO_2	20 ZrO_2/ZrO_2
773	84	80	73	62	78	72	65
873	70	60	66	54	66	70	63
973	48	56	63	52	55	68	62
1073	20	33	40	51	35	32	47

The fresh 20 CeO_2/ZrO_2 and 20 ZrO_2/ZrO_2 samples, calcined at only 773 K, had lower surface areas, 62 m^2/g and 65 m^2/g, respectively, primarily because of the added mass of the films. For example, the addition of 0.3 g ZrO_2/g ZrO_2 would decrease the specific surface area by a factor of 1.3 (84 m^2/1.30 g = 63 m^2/g), even if the film had no influence on the pore sizes or distribution. Similar to what was reported for ZrO_2 ALD films on CeO_2, the decrease in surface areas with calcination temperature was much less severe for both the 20 CeO_2/ZrO_2 and 20 ZrO_2/ZrO_2 samples compared to pure ZrO_2. Following calcination to 1073 K, the surface areas of these two samples were 51 and 47 m^2/g, respectively, more than double that of the unmodified sample that had been heated to this temperature. The effects of ALD modification were also observed, to a lesser extent, with 10 and 2 ALD cycles of both CeO_2 and ZrO_2.

Another indication of the stabilizing effect of the ALD films comes from the XRD patterns shown in Figure 2. The patterns in Figure 2a are of the pure ZrO_2, 20 CeO_2/ZrO_2, and 20 ZrO_2/ZrO_2 samples after calcination at 773 K. The pattern for pure ZrO_2 indicates that the material is primarily in the tetragonal form, as shown by the large peak at 30 degrees 2θ, but with a small amount of monoclinic phase, shown by the small peak near 28 degrees 2θ. The deposition of 20 ALD cycles of either CeO_2 or ZrO_2, with calcination at 773 K, did not change the patterns. While peaks associated with crystalline CeO_2 would be difficult to distinguish from the mixture of tetragonal and monoclinic ZrO_2, previous work has shown that ALD films this thin (the film on the 20 CeO_2/ZrO_2 sample is only 0.33 nm thick) are invisible to XRD [20]. The effects of calcining the same three samples to 1073 K is shown in Figure 2b. The pure ZrO_2 is almost completely converted to its monoclinic form. By contrast, the 20 CeO_2/ZrO_2 remains primarily in the tetragonal form and the 20 ZrO_2/ZrO_2 sample is a mixture of the two phases.

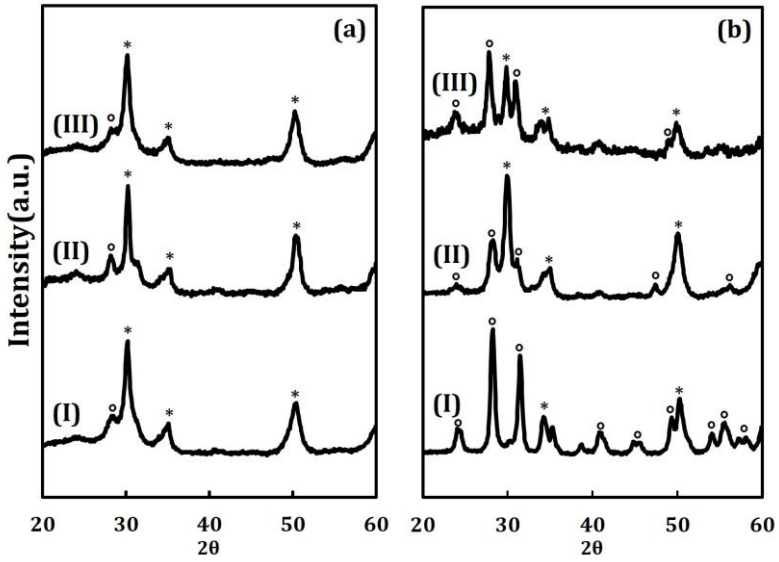

Figure 2. XRD patterns for (**I**) unmodified ZrO_2, (**II**) 20 CeO_2/ZrO_2, and (**III**) 20 ZrO_2/ZrO_2. Patterns shown in (**a**) were from samples calcined at 773 K and patterns in (**b**) at 1073 K. Peaks marked with asterisks stand for tetragonal phase ZrO_2 and open circles stand for monoclinic phase ZrO_2.

The sintering character of powders is critically important in ceramics processing [21], and the BET and XRD results suggested that ALD modification should significantly affect the properties of ZrO_2 powder. That this is the case is demonstrated by Figure 3, which plots the percent change in the diameters of ZrO_2, 20 CeO_2/ZrO_2, and 20 ZrO_2/ZrO_2 wafers as a function of calcination temperature. Not surprisingly, the ultimate shrinkage after calcination to 1573 K was the same for each of the materials: ~16%; however, pure ZrO_2 had sintered to this value by 1273 K. The sintering curves for the ALD-modified samples, especially 20 CeO_2/ZrO_2, were shifted upward by approximately 100 K, which means that the ALD-prepared samples would only have the same shrinkage if heated an additional 100 K, again consistent with the fact that the ALD films had increased the stability of the powders.

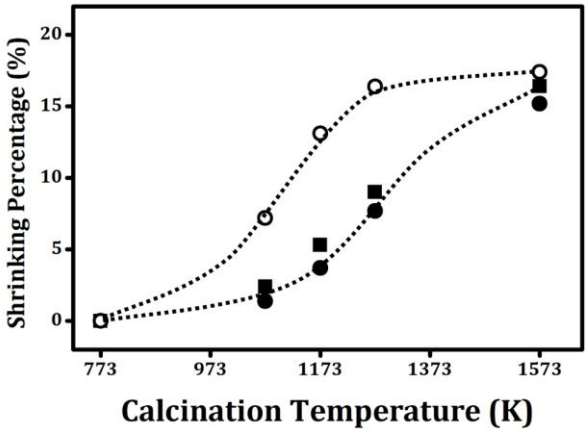

Figure 3. Shrinkage of ceramic wafers as a function of calcination temperature: (○) Unmodified ZrO_2; (■) 20 CeO_2/ZrO_2; (●) 20 ZrO_2/ZrO_2. The original diameters for all the pellets were 1.495 cm.

It has been previously demonstrated that rates for CO oxidation at interfacial sites between Pd and CeO_2 are much higher than rates on either Pd or CeO_2 individually [22]. There is no similar enhancement of CO-oxidation rates at Pd and zirconia interfaces [8]. Therefore, to determine how the ALD-modified catalysts would perform as catalyst supports and obtain a measure of how good

the contact between Pd and the ceria in the samples is, we measured CO-oxidation rates on selected samples after adding 1 wt % Pd. Measurements were performed on the ZrO_2, CeO_2, 20 CeO_2/ZrO_2, and 20 ZrO_2/ZrO_2 samples after the supports had been calcined to either 773 K or 1073 K. In all cases, the Pd was added after calcination of the support. After the addition of Pd, the catalysts were calcined to 773 K. Pd dispersions for each of the catalysts are reported in Table 2. It is interesting to notice that the dispersions measured for Pd/CeO_2 and $Pd/20CeO_2/ZrO_2$ were similar and significantly higher than those on the Pd/ZrO_2 and $Pd/20ZrO_2/ZrO_2$ samples, which implies that there is a more favorable interaction between the Pd and the CeO_2.

Table 2. Pd dispersions as a function of support calcination temperature.

Calcination Temperature (K)	Pd Dispersion (%)			
	ZrO_2	20 ZrO_2/ZrO_2	CeO_2	20 CeO_2/ZrO_2
773 K	6.3	13.2	39.6	38.4
1073 K	4.7	11.2	30.1	32.3

Figure 4a shows differential reaction rates for the catalysts after the supports had been calcined to 773 K. Rates on the Pd/ZrO_2 and $Pd/20ZrO_2/ZrO_2$ catalysts were essentially identical and rates on the Pd/CeO_2 and $Pd/20CeO_2/ZrO_2$ were essentially identical. Extrapolating the rates to the same temperature, rates on the two ceria-containing samples were more than a factor of ten higher, which is more than can be explained by the higher dispersions. This agrees with the previous observations of enhanced rates at the Pd–ceria interface. Figure 4b shows differential rates for the same materials after the supports had been calcined to 1073 K. The only catalyst affected by this treatment was the Pd/CeO_2 sample. The loss of activity in this sample is likely due to loss of the CeO_2 surface area, as reported previously for a similar Pd/CeO_2 catalyst used for the WGS reaction [23]. The Pd/ZrO_2 and $Pd/20ZrO_2/ZrO_2$ catalysts were not affected because the reaction only occurs on the Pd phase. The $Pd/20CeO_2/ZrO_2$ catalyst was not affected because the surface area did not significantly change.

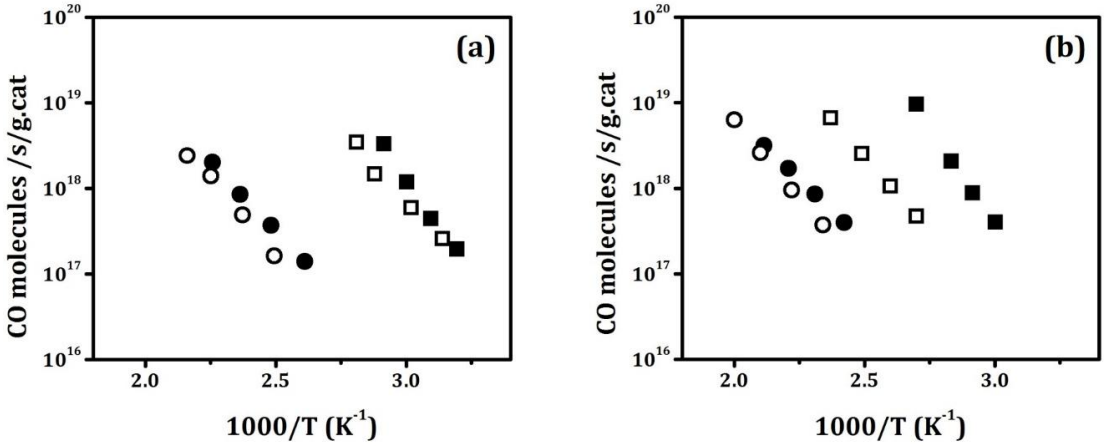

Figure 4. Differential CO oxidation for various samples after the addition of 1 wt % Pd. The samples in (**a**) were calcined to 773 K and the samples in (**b**) to 1073 K. Pd was added after calcination. The samples are as follows: (■) 20 CeO_2/ZrO_2; (●) 20 ZrO_2/ZrO_2; (○) unmodified ZrO_2; (□) unmodified CeO_2.

The present results expand on the previous report showing that the ALD of very thin films of ZrO_2 on CeO_2 are able to stabilize the surface area and structure of the CeO_2 substrate. We have shown here that substrate stabilization by ALD is not unique to ZrO_2 films on CeO_2. In particular, the fact that ZrO_2 films are able to stabilize ZrO_2 substrates implies that the effect must be structural and not due to any chemical bonding effects between different species. Finally, it is noteworthy that there is a

noticeable change in the sintering characteristics following only two ALD cycles, corresponding to a coverage that is much less than a monolayer.

Since cation surface diffusion is a major contributor to the sintering process in ceramic materials [24], it would appear that ALD films act by suppressing surface diffusion. The mechanism behind this suppression may be different depending on the system. In the case of CeO_2 films on ZrO_2, there may be bonding between the dissimilar atoms that stabilize the surface cations. With ZrO_2 films on ZrO_2, the role of the ALD film may be to remove hydroxyls or fill in vacancies, thus stabilizing the metal cations.

In addition to stabilizing the surface area, the ALD films influenced the structure of the zirconia substrate (e.g., preventing the formation of the monoclinic phase upon heating). This can be important in some catalytic applications. For example, the acid-base properties of zirconia are reported to change with the different polymorphs [25]. The ability to stabilize a particular phase without significantly changing the surface area and without the addition of dopants could be very useful.

ALD thin films can also be useful in making high-surface-area, functional supports. The present CO-oxidation results indicate that a CeO_2 ALD film as thin as 0.34 nm can increase rates for CO oxidation on supported-Pd catalysts to the same level observed for Pd supported on CeO_2. It is difficult to maintain CeO_2 powders in a high-surface-area form. The fact that one can achieve similar properties in a thin film catalyst opens up the possibility of using a more stable substrate for an enhanced surface area, while still having the high catalytic activity of the functional oxide. The use of thin-film supports could also be very important if the functional oxide is expensive.

While there is a growing excitement over the use of ALD in catalyst preparation [26,27], it is clear that we are still learning how to take full advantage of the approach for producing the best materials. The fact that ALD can affect the stability and structure of catalysts supports adds another factor to the potential advantages.

3. Experimental Methods

CeO_2 and ZrO_2 powders were prepared by precipitating aqueous solutions of either zirconyl nitrate hydrate (5 g, $ZrO(NO_3)_2{\cdot}xH_2O$, 99%, Sigma-Aldrich, St. Louis, MO, USA) or $Ce(NO_3)_2{\cdot}6H_2O$ (Sigma Aldrich, St. Louis, MO, USA) with excess ammonium hydroxide (NH_4OH, Fisher Scientific, Waltham, MA, USA). The resulting precipitates were then dried overnight at 333 K and heated in air at 773 K for 3 h. After this pretreatment, the ZrO_2 powder had a BET surface area of 84 m^2/g and the CeO_2 powder had a surface area of 59 m^2/g.

ALD modification was performed using procedures and equipment that have been described in previous publications [19,28]. Briefly, the homebuilt ALD system consists of two heated chambers, one for the powder that was to be modified and one for the organometallic precursor, both of which could be evacuated with a mechanical vacuum pump. First, the powder was first heated to 503 K in a vacuum, after which it was exposed to ~5 Torr of the organometallic precursor, either $Zr(TMHD)_4$ (Tetrakis(2,2,6,6-tetramethyl-3,5-heptanedionato) zirconium(IV), 99%, Strem, Newburyport, MA, USA) or $Ce(TMHD)_4$ (Tetrakis(2,2,6,6-tetramethyl-3,5-heptanedionato) cerium(IV)), for 300 s. To ensure that the substrate surface was saturated with adsorbed precursor, the substrate was exposed to the precursors multiple times before evacuation.

To determine the conditions required to remove the organic ligands from the adsorbed precursor, temperature-programmed oxidation was performed on the ZrO_2 powder following exposure to $Ce(TMHD)_4$, and the results are shown in Figure 5. This experiment was performed in flowing air with 0.1 g of sample, a heating rate of 20 K/min, an air flowrate of 50 mL/min, and a mass spectrometer to monitor the CO_2 produced by the oxidation reaction. The data show that temperatures in excess of 600 K are required to completely remove the ligands.

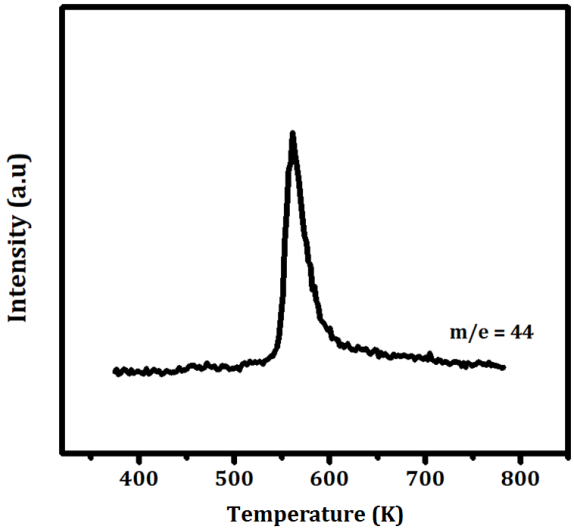

Figure 5. Temperature-programmed oxidation performed on the ZrO_2 after exposure to the $Ce(TMHD)_4$ precursor. The heating rate for the sample was 20 K/min.

Because the TMHD ligands were not completely oxidized at 503 K [28], the samples in this study were removed from the ALD system after each precursor exposure and heated to 773 K for 300 s in a muffle furnace. The samples were then placed into the ALD system again and the cycle repeated. The total time for one cycle, including exposure, evacuation, and oxidation cycles, was approximately 12 min. Film growth rates were determined from changes in the sample mass using an electronic scale with a precision of 0.1 mg. Sensitivity was not a problem because a simple calculation shows that a uniform, 0.1 nm thick CeO_2 film on 84 m^2/g ZrO_2 will increase the sample mass by 6% [18]. ZrO_2 samples modified by ALD will be referred to by the species deposited and the number of ALD cycles (e.g., a sample with 20 ALD cycles of CeO_2 is referred to as 20 CeO_2/ZrO_2).

Surface areas were measured using BET isotherms in a homemade adsorption apparatus. For each sample, the surface area was measured 3 times and the surface areas were found to vary by no more than 2 m^2/g. X-ray diffraction (XRD) patterns were recorded on a Rigaku Smartlab diffractometer equipped with a Cu Kα source (λ = 0.15416 nm).

Pd with a concentration of 1 wt % was added to selected samples using incipient wetness of aqueous solutions of tetraamminepalladium nitrate (5.0% $Pd(NH_3)_4(NO_3)_2$, Alfa Aesar). After impregnation of the Pd salt, the samples were dried overnight at 333 K and calcined in air at 773 K for 1 h. Pd dispersions were measured volumetrically using CO adsorption uptakes at room temperature, assuming adsorption of 1 CO molecule per Pd surface atom. The adsorption was performed on samples that were first reduced in 200 Torr H_2 at 423 K.

CO oxidation rates were measured at differential conversions in a tubular flow reactor, using a gas chromatograph (SRI8610C) equipped with a Hayesep Q column and a TCD detector to measure effluent concentrations. The total gas flow rate through the reactor was 120 $mL \cdot min^{-1}$, and sample size was 0.10 g in all experiments. The partial pressures of CO and O_2 were fixed at 25 and 12.5 Torr, respectively, by adjusting the flow rates of CO, O_2, and He.

The sintering character of the powders was examined by measuring the diameters of pressed wafers that had been heated to various temperatures. In these experiments, 0.1600 g of each sample were pressed into a wafer that had an initial diameter of 1.495 cm. The samples were then calcined for 30 min to various temperatures. The diameters of the pellets were then measured by Vernier caliper with the precision of 0.005 cm.

4. Conclusions

ALD films of CeO_2 and ZrO_2 on ZrO_2 powders are able to significantly stabilize the surface area and zirconia phase by suppressing surface diffusion of cations. CeO_2 films can also enhance the catalytic properties of the ZrO_2 when the material is used as a support for Pd in CO oxidation. This ability to modify oxides by ALD could have important for applications involving CeO_2 catalysts.

Acknowledgments: We are grateful to the Department of Energy, Office of Basic Energy Sciences, Chemical Sciences, Geosciences and Biosciences Division, Grant No. DE-FG02-13ER16380 for support of this work.

Author Contributions: Chao Lin and Tzia Ming Onn conceived and designed the experiments; Chao Lin, Xinyu Mao, Tzia Ming Onn, and Joonbaek Jang performed the experiments; Chao Lin, Xinyu Mao, Tzia Ming Onn, and Joonbaek Jang analyzed the data; Raymond J. Gorte and Chao Lin wrote the manuscript.

Conflicts of Interest: The authors declare no conflict of interest.

References

1. Gorte, R.J. Ceria in Catalysis: From Automotive Applications to the Water–Gas Shift Reaction. *AIChE J.* **2010**, *56*, 1126–1135. [CrossRef]
2. Fu, Q.; Saltsburg, H.; Flytzani-Stephanopoulos, M. Active nonmetallic Au and Pt species on ceria-based water-gas shift catalysts. *Science* **2003**, *301*, 935–938. [CrossRef] [PubMed]
3. Trovarelli, A. Catalytic properties of ceria and CeO_2-containing materials. *Catal. Rev. Sci. Eng.* **1996**, *38*, 439–520. [CrossRef]
4. Jacobs, G.; Graham, U.M.; Chenu, E.; Patterson, P.M.; Dozier, A.; Davis, B.H. Low-temperature water–gas shift: Impact of Pt promoter loading on the partial reduction of ceria and consequences for catalyst design. *J. Catal.* **2005**, *229*, 499–512. [CrossRef]
5. Montini, T.; Melchionna, M.; Monai, M.; Fornasiero, P. Fundamentals and catalytic applications of CeO_2-based materials. *Chem. Rev.* **2016**, *116*, 5987–6041. [CrossRef] [PubMed]
6. Oh, S.H.; Mitchell, P.J.; Siewert, R.M. Methane oxidation over alumina-supported noble metal catalysts with and without cerium additives. *J. Catal.* **1991**, *132*, 287–301. [CrossRef]
7. Zhou, G.; Shah, P.R.; Kim, T.; Fornasiero, P.; Gorte, R.J. Oxidation entropies and enthalpies of ceria–zirconia solid solutions. *Catal. Today* **2007**, *123*, 86–93. [CrossRef]
8. Bunluesin, T.; Gorte, R.J.; Graham, G.W. CO Oxidation for the Characterization of Reducibility in Oxygen Storage Components of Three-Way Automotive Catalysts. *Appl. Catal. B* **1997**, *14*, 105–115. [CrossRef]
9. Kim, T.; Vohs, J.M.; Gorte, R.J. Thermodynamic Investigation of the Redox Properties of Ceria-Zirconia Solid Solutions. *Ind. Eng. Chem. Res.* **2006**, *45*, 5561–5565. [CrossRef]
10. Aneggi, E.; Boaro, M.; de Leitenburg, C.; Dolcetti, G.; Trovarelli, A. Insights into the redox properties of ceria-based oxides and their implications in catalysis. *J. Alloys Compd.* **2006**, *408*, 1096–1102. [CrossRef]
11. Dutta, G.; Waghmare, U.V.; Baidya, T.; Hegde, M.; Priolkar, K.; Sarode, P. Reducibility of $Ce_{1-x}Zr_xO_2$: Origin of enhanced oxygen storage capacity. *Catal. Lett.* **2006**, *108*, 165–172. [CrossRef]
12. He, B.J.J.; Wang, C.X.; Zheng, T.T.; Zhao, Y.K. Thermally Induced Deactivation and the Corresponding Strategies for Improving Durability in Automotive Three-Way Catalysts. *Johns. Matthey Technol. Rev.* **2016**, *60*, 196–203. [CrossRef]
13. Shah, P.R.; Kim, T.; Zhou, G.; Fornasiero, P.; Gorte, R.J. Evidence for Entropy Effects in the Reduction of Ceria-Zirconia Solutions. *Chem. Mater.* **2006**, *18*, 5363–5369. [CrossRef]
14. Trovarelli, A. Structural and oxygen storage/release properties of CeO_2-based solid solutions. *Comments Inorg. Chem.* **1999**, *20*, 263–284. [CrossRef]
15. Putna, E.S.; Vohs, J.M.; Gorte, R.J. Characterization of Ceria Films on α-Al_2O_3 (0001) and Polycrystalline Zirconia Using O_2 TPD with Labeled $^{18}O_2$. *Catal. Lett.* **1997**, *45*, 143–147. [CrossRef]
16. Song, K.; Schmid, H.; Srot, V.; Gilardi, E.; Gregori, G.; Du, K.; Maier, J.; van Aken, P.A. Cerium Reduction at the Interface between Ceria and Yttria-Stabilized Zirconia and Implications for Interfacial Oxygen Non-stoichiometry. *APL Mater.* **2014**, *2*, 032104. [CrossRef]
17. Costa-Nunes, O.; Ferrizz, R.M.; Gorte, R.J.; Vohs, J.M. Structure and Thermal Stability of Ceria Films Supported on YSZ (100) and α-Al_2O_3 (0001). *Surf. Sci.* **2005**, *592*, 8–17. [CrossRef]

18. Onn, T.M.; Arroyo-Ramirez, L.; Monai, M.; Oh, T.-S.; Talati, M.; Fornasiero, P.; Gorte, R.J.; Khader, M.M. Modification of Pd/CeO_2 Catalyst by Atomic Layer Deposition of ZrO_2. *Appl. Catal. B* **2016**, *197*, 280–285. [CrossRef]
19. Onn, T.M.; Dai, S.; Chen, J.; Pan, X.; Graham, G.W.; Gorte, R.J. High-Surface Area Ceria–Zirconia Films Prepared by Atomic Layer Deposition. *Catal. Lett.* **2017**, *147*, 1464–1470. [CrossRef]
20. Onn, T.M.; Zhang, S.; Arroyo-Ramirez, L.; Chung, Y.-C.; Graham, G.W.; Pan, X.; Gorte, R.J. Improved thermal stability and methane-oxidation activity of Pd/Al_2O_3 catalysts by atomic layer deposition of ZrO_2. *ACS Catal.* **2015**, *5*, 5696–5701. [CrossRef]
21. Mistler, R.E.; Twiname, E.R. *Tape Casting: Theory and Practice*; The American Ceramic Society: Westerville, OH, USA, 2000.
22. Cargnello, M.; Doan-Nguyen, V.V.; Gordon, T.R.; Diaz, R.E.; Stach, E.A.; Gorte, R.J.; Fornasiero, P.; Murray, C.B. Control of Metal Nanocrystal Size Reveals Metal-Support Interface Role for Ceria Catalysts. *Science* **2013**, *341*, 771–773. [CrossRef] [PubMed]
23. Onn, T.M.; Zhang, S.; Arroyo-Ramirez, L.; Xia, Y.; Wang, C.; Pan, X.; Graham, G.W.; Gorte, R.J. High-Surface-Area Ceria Prepared by ALD on Al_2O_3 Support. *Appl. Catal. B* **2017**, *201*, 430–437. [CrossRef]
24. Wakai, F.; Brakke, K. Mechanics of sintering for coupled grain boundary and surface diffusion. *Acta Mater.* **2011**, *59*, 5379–5387. [CrossRef]
25. Gonell, F.; Portehault, D.; Julián-López, B.; Vallé, K.; Sanchez, C.; Corma, A. One step microwave-assisted synthesis of nanocrystalline WO_x–ZrO_2 acid catalysts. *Catal. Sci. Technol.* **2016**, *6*, 8257–8267. [CrossRef]
26. Yang, N.; Yoo, J.S.; Schumann, J.; Bothra, P.; Singh, J.A.; Valle, E.; Abild-Pedersen, F.; Norskov, J.K.; Bent, S.F. Rh–MnO interface sites formed by atomic layer deposition promote syngas conversion to higher oxygenates. *Chem. Biomol. Eng.* **2017**, *8*, 41–62. [CrossRef]
27. O'Neill, B.J.; Jackson, D.H.; Lee, J.; Canlas, C.; Stair, P.C.; Marshall, C.L.; Elam, J.W.; Kuech, T.F.; Dumesic, J.A.; Huber, G.W. Catalyst design with atomic layer deposition. *ACS Catal.* **2015**, *5*, 1804–1825. [CrossRef]
28. Anthony, S.Y.; Küngas, R.; Vohs, J.M.; Gorte, R.J. Modification of SOFC cathodes by atomic layer deposition. *J. Electrochem. Soc.* **2013**, *160*, F1225–F1231.